

Resolution enhancement of images pair based on block cross interpolation

Oday Jasim Mohammed Al-Furaiji

Dept. Computer Science, Shatt Al-Arab University College, Basra, Iraq

Abstract

The image resolution enhancement concerns with the improvement of image resolution based on merging of several acquisitions of low-resolution observations by camera. In this paper, an algorithm for increasing the resolution of two images shifted by half a pixel horizontally and vertically is proposed, based on block cross-interpolation. The algorithm aims at reducing the errors in the known (bicubic and averaging) methods, using the criteria of MSE and PSNR.

Keywords: PSNR, MSE, Block cross-interpolation; Bicubic interpolation

Corresponding Author:

Author Name, **Oday Jasim Mohammed Al-Furaiji**

Departement, Computer Science

University , Shatt Al-Arab University

Address. Basra, Iraq

E-mail: odaymohammed@mail.ru

1. Introduction

Image resolution depends on the physical characteristics of the sensor: the optical properties, density and spatial response of the sensor components. Increasing the resolution by sensor adjustment may not be an existing choice. In most known methods of subpixel processing, one image or several images are considered as the raw data, the relative pixel shift between them is precisely unknown (un-normalized) [1-8]. By using a moving video camera, images can be formed that are shifted by half a pixel horizontally and vertically, for example, down and to the right, which are the raw data for subpixel processing[9-13]. To enhance the resolution of such images, two main approaches are of interest: based on gradient analysis in overlapping neighborhoods, self-similarity and regularization (nonlinear methods) and based on interpolation and averaging (linear methods). The first approach provides less errors, but requires considerable resources. The second approach is characterized by low computational complexity, but it leads to smoothing of sharp changes in brightness in the region of contours and blurring of small artifacts[14-23].

The aim of the work is to develop a computationally simple algorithm for increasing the resolution of two images shifted by half a pixel horizontally and vertically, providing a reduction in errors in comparison with algorithms based on bicubic interpolation and averaging.

2. Algorithm of block cross-interpolation of a pair of images

An algorithm for increasing the resolution of two images shifted by half a pixel horizontally and vertically is submitted, on the basis of block cross-interpolation. The essence of the algorithm consists in splitting each initial image into overlapping blocks of 2×2 pixels in size such that for each pixel of one image there are four pixels (a pixel block) of another image "Fig. 1", and based on the brightness values of each pixel of each image, is formed a new block of pixels that do not overlap with other blocks.

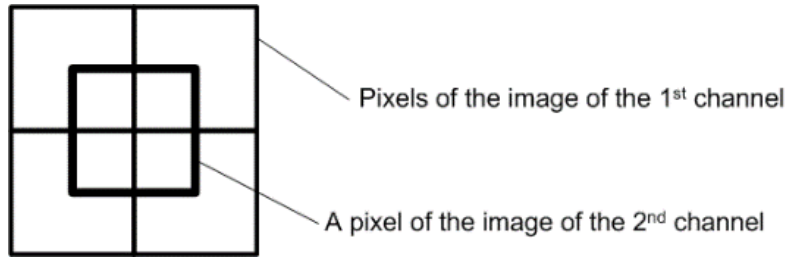


Figure 1. Shifting the pixels of initial images

The block cross-interpolation algorithm consists of the following steps.

1) Processing the pixels of the first initial image.

1.1) Selecting the pixel $i_1(y, x)$ of the first initial image $I_1 = \|i_1(y, x)\|_{(y=0, \overline{Y-1}, x=0, \overline{X-1})}$ at $y = \overline{1, Y-2}$, $x = \overline{1, X-2}$.

1.2) For the pixel $i_1(y, x)$ of image I_1 is calculated total brightness $s_1(y, x)$ corresponding to pixels blocks $\{i_2(y-1, x-1), i_2(y-1, x), i_2(y, x-1), i_2(y, x)\}$ of the second initial image $I_2 = \|i_2(y, x)\|_{(y=0, \overline{Y-1}, x=0, \overline{X-1})}$ using the expression

$$s_1(y, x) = \sum_{m=-1}^0 \sum_{n=-1}^0 i_2(y-m, x-n)$$

at $y = \overline{1, Y-2}$, $x = \overline{1, X-2}$.

1.3) Forming the first intermediate interpolated image $\tilde{I}_1 = \|\tilde{i}_1(y, x)\|_{(y=0, \overline{2Y-1}, x=0, \overline{2X-1})}$, and the pixels values $\{\tilde{i}_1(2y, 2x), \tilde{i}_1(2y+1, 2x), \tilde{i}_1(2y, 2x+1), \tilde{i}_1(2y+1, 2x+1)\}$ in blocks of which are calculated using the expression

$$\tilde{i}_1(2y+m, 2x+n) = 4i_1(y, x) \frac{i_2(y-1+m, x-1+n)}{s_1(y, x)}$$

at $m = \overline{0, 1}$, $n = \overline{0, 1}$, $y = \overline{1, Y-2}$, $x = \overline{1, X-2}$.

2) Processing of the second initial image pixels

$$I_2 = \|i_2(y, x)\|_{(y=0, \overline{Y-1}, x=0, \overline{X-1})}$$

2.1) Selecting the pixel $i_2(y, x)$ of the second initial image $I_2 = \|i_2(y, x)\|_{(y=0, \overline{Y-1}, x=0, \overline{X-1})}$ at $y = \overline{1, Y-2}$, $x = \overline{1, X-2}$.

2.2) For the pixel $i_2(y, x)$ of image I_2 is calculated total brightness $s_2(y, x)$ corresponding to pixels blocks $\{i_1(y-1, x-1), i_1(y-1, x), i_1(y, x-1), i_1(y, x)\}$ of the first initial image $I_1 = \|i_1(y, x)\|_{(y=0, \overline{Y-1}, x=0, \overline{X-1})}$ using the expression

$$s_2(y, x) = \sum_{m=-1}^0 \sum_{n=-1}^0 i_1(y-m, x-n)$$

at $y = \overline{1, Y-2}$, $x = \overline{1, X-2}$.

2.3) Forming the second intermediate interpolated image $\tilde{I}_2 = \|\tilde{i}_2(y, x)\|_{(y=0, \overline{2Y-1}, x=0, \overline{2X-1})}$, and the pixels values $\{\tilde{i}_2(2y, 2x), \tilde{i}_2(2y+1, 2x), \tilde{i}_2(2y, 2x+1), \tilde{i}_2(2y+1, 2x+1)\}$ in blocks of which are calculated using the expression

$$\tilde{i}_2(2y+m, 2x+n) = 4i_2(y, x) \frac{i_1(y-1+m, x-1+n)}{s_2(y, x)}$$

at $m = \overline{0, 1}$, $n = \overline{0, 1}$, $y = \overline{1, Y-2}$, $x = \overline{1, X-2}$.

3) Forming the resulting high-resolution image $\hat{I} = \|\hat{i}(y, x)\|_{(y=0, \overline{2Y-1}, x=0, \overline{2X-1})}$ as a result of pixel averaging of the first \tilde{I}_1 and second \tilde{I}_2 intermediate interpolated images using the expression

$$\hat{i}(y, x) = \frac{\tilde{i}_1(y, x) + \tilde{i}_2(y, x)}{2}$$

at $y = \overline{1, 2Y-1}, x = \overline{1, 2X-1}$.

The computational complexity of this algorithm is estimated at approximately 27 operations per pixel of the resulting high-resolution image.

The scheme of the block cross-interpolation of images is shown in “Fig. 2”. The scheme consists of two channels in which on the basis of two low-resolution initial images are formed two intermediate images of increased resolution, and then the results of channel-by-channel processing are combined to form the resulting high-resolution image. The amount of data processed within each channel is limited to 9 pixels (4 pixels of one channel and 1 pixel of the second channel at the input and 4 pixels at the output). The amount of data processed when combining the results of channel-by-channel processing is 3 pixels (2 pixels at the inputs and 1 pixel at the output).

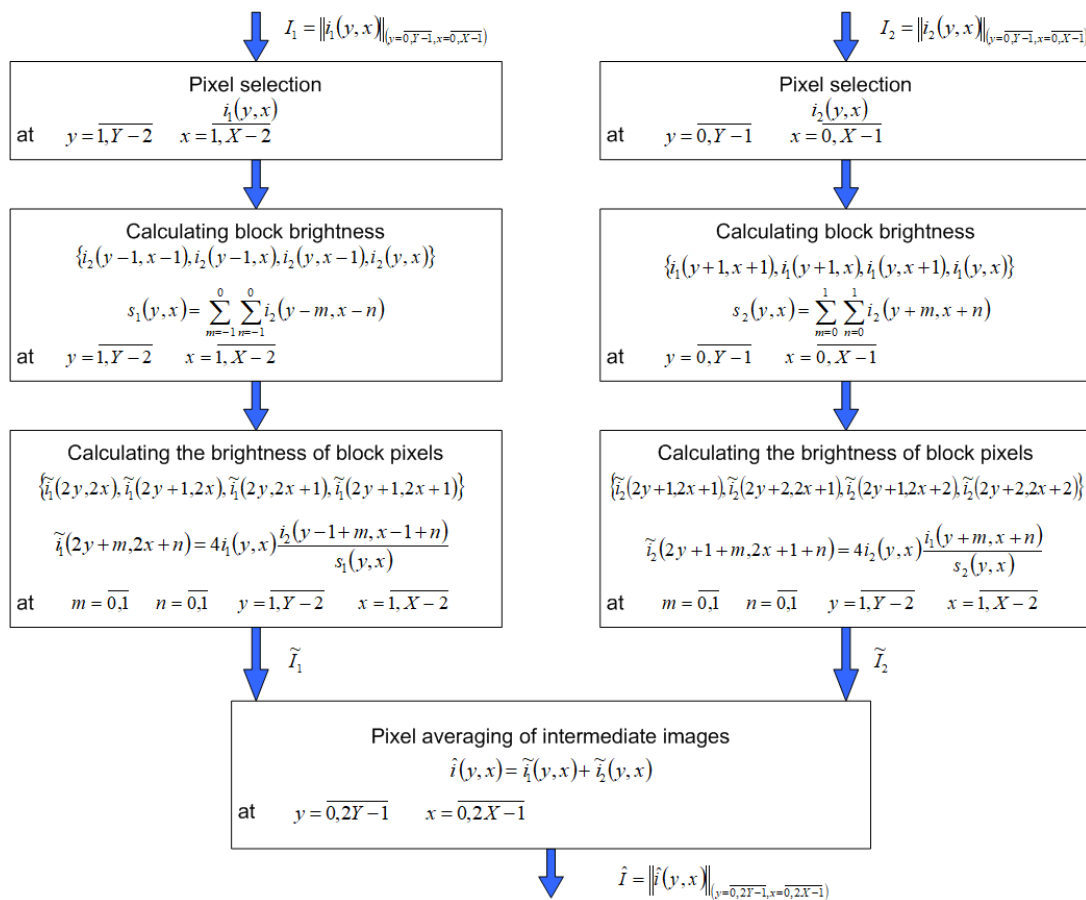


Figure 2. Scheme of block cross-interpolation of images

In the block cross-interpolation algorithm, the errors are due to inaccuracies in the brightness distribution within the block of pixels. Therefore, errors are grouped on high-frequency sections of images (on textures and near contours).

3. The effectiveness of block cross-interpolation evaluation

Figure 3 shows the pairs of test images that are displaced relative to each other by half a pixel vertically and horizontally.

Figure 4 shows the equivalent high-resolution test reference images gained by a high-resolution video camera. In Figures 5 – 7 are shown high resolution images obtained as a result of processing test images using the block cross-interpolation algorithm, as well as bicubic interpolation and averaging algorithms.

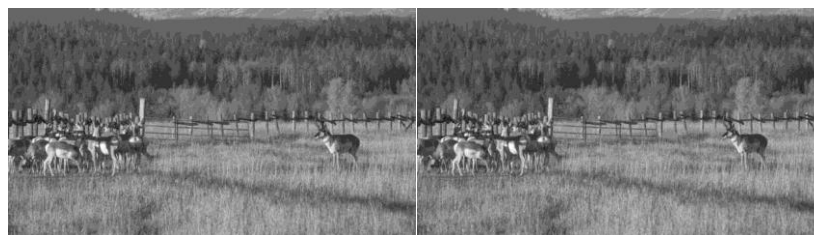
Figure 4 shows the equivalent high-resolution test reference images gained by a high-resolution video camera. In Figures 5 – 7 are shown high resolution images obtained as a result of processing test images using the block cross-interpolation algorithm, as well as bicubic interpolation and averaging algorithms.



a) Pairs of image 1



b) Pairs of image 2



c) Pairs of image 3



d) Pairs of image 4



e) Pairs of image 5

Figure 3. The pairs of test images (1,2,3,4,5) that are shifted relative to each other by half a pixel vertically and horizontally



a) image 1

b) image 2



c) image 3

d) image 4



e) image 5

Figure 4. Test images (1,2,3,4,5) of high resolution



a) image 1

b) image 2



c) image 3

d) image 4



e) image 5

Figure 5. High-resolution images generated by block cross-interpolation



a) image 1

b) image 2



c) image 3

d) image 4



e) image 5

Figure 5. High-resolution images generated by averaging



a) image 1

b) image 2

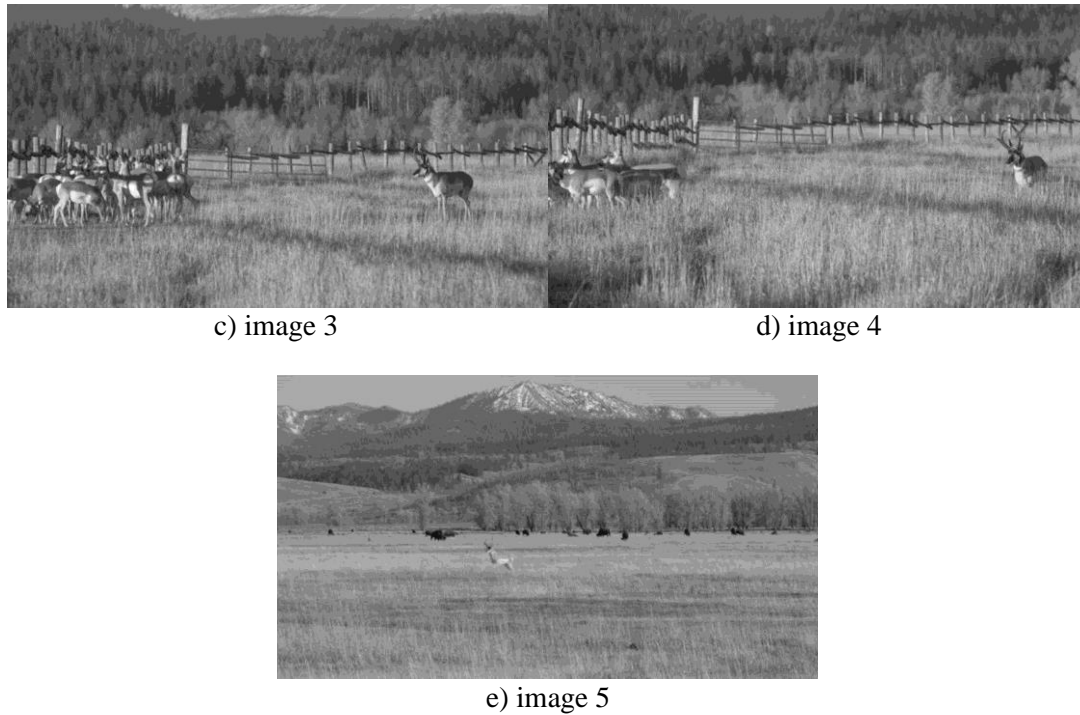


Figure 6. Images of high-resolution generated by bicubic interpolation

In Table 1 is shown the mean square error MSE and the peak signal-to-noise ratio PSNR for high-resolution test reference images and high-resolution resulting images obtained using the algorithms of block cross-interpolation, bicubic interpolation, and averaging. The values of these parameters are determined using the expressions

$$MSE = \frac{1}{YX} \sum_{y=0}^{Y-1} \sum_{x=0}^{X-1} (i(y,x) - \hat{i}(y,x))^2$$

$$PSNR = 10 \lg \left(\frac{255^2}{MSE} \right)$$

where $i(y,x)$ – are the pixels of test reference image.

From Table 1 it follows that block cross-interpolation provides a reduction in the mean square error by approximately 3.3891 and 2.2140 times (an increase in the signal-to-noise ratio by about 5 dB and 3 dB) compared to averaging and bicubic interpolation, respectively.

Table 1. Interpolation methods characteristics

Interpolation method	MSE/PSNR (dB)					Average MSE/PSNR (dB)
	Image1	Image2	Image3	Image4	Image5	
Block cross	7.74/39.24	20.67/34.98	14.03/36.66	11.15/37.66	16.39/35.98	13.99/36.90
Averaging	19.76/35.17	71.14/29.61	55.25/30.71	63.15/30.13	27.85/33.68	47.43/31.8599
Bicubic	11.99/37.34	48.31/31.29	34.44/32.76	39.93/32.11	20.25/35.06	30.98/33.71

4. Conclusion

In this paper, an algorithm for increasing the resolution of two images shifted by half a pixel horizontally and vertically is proposed, based on block cross-interpolation using 2x2 pixel blocks. It is shown that block cross-interpolation provides a reduction in the mean square error MSE of an average 3.3891 and 2.2140 times (an increase in the signal-to-noise ratio by approximately 5 dB and 3 dB) compared to averaging and bicubic interpolation, respectively.

References

- [1] S. Shinde, M. J. I. J. o. C. S. Dewangan, and E. Survey, "Single Image Improvement using Superresolution," vol. 3, no. 2, p. 47, 2012.
- [2] W.-l. Chen, L. Guo, and W.-l. J. J. Xia, "A Novel Super-resolution Reconstruction Algorithm Based on Subspace Projection," vol. 8, no. 8, pp. 1893-1897, 2013.
- [3] H. T. S. Al-Rikabi, *Enhancement of the MIMO-OFDM Technologies*. California State University, Fullerton, 2013.
- [4] J. Song and F. Wang, "Image Super-Resolution Reconstruction Based on Multi-scale Convolutional Neural Network," in *International Conference on Genetic and Evolutionary Computing*, 2019, pp. 389-398: Springer.
- [5] K. Zhang, Z. Wang, J. Li, X. Gao, and Z. J. S. P. Xiong, "Learning recurrent residual regressors for single image super-resolution," vol. 154, pp. 324-337, 2019.
- [6] Z. Hu *et al.*, "Super-resolution of PET image based on dictionary learning and random forests," vol. 927, pp. 320-329, 2019.
- [7] H. T. Alrikabi, A. H. M. Alaidi, A. S. Abdalrada, and F. T. J. I. J. o. E. T. i. L. Abed, "Analysis the Efficient Energy Prediction for 5G Wireless Communication Technologies," vol. 14, no. 08, pp. 23-37, 2019.
- [8] C. S. Ike, N. J. P. A. Muhammad, and Applications, "Separable property-based super-resolution of lousy image data," pp. 1-14, 2019.
- [9] M. Nixon, F. Outlaw, L. W. MacDonald, and T. S. Leung, "The importance of a device specific calibration for smartphone colorimetry," in *Color and Imaging Conference*, 2019, vol. 2019, no. 1, pp. 49-54: Society for Imaging Science and Technology.
- [10] A. Punnappurath and M. S. Brown, "Reflection removal using a dual-pixel sensor," in *Proceedings of the IEEE Conference on Computer Vision and Pattern Recognition*, 2019, pp. 1556-1565.
- [11] H. Alrikabi, A. H. Alaidi, and K. J. I. J. o. I. M. T. Nasser, "The Application of Wireless Communication in IOT for Saving Electrical Energy," vol. 14, no. 01, pp. 152-160, 2020.
- [12] C. Saunders, J. Murray-Bruce, and V. K. J. N. Goyal, "Computational periscopy with an ordinary digital camera," vol. 565, no. 7740, pp. 472-475, 2019.
- [13] M. Yoshida, T. Sonoda, H. Nagahara, K. Endo, Y. Sugiyama, and R.-I. J. I. T. o. C. I. Taniguchi, "High-Speed Imaging using CMOS Image Sensor with Quasi Pixel-Wise Exposure," 2019.
- [14] K. Basak and S. Mandal, "Multiscale Signal Processing Methods for Improving Image Reconstruction and Visual Quality in LED-Based Photoacoustic Systems," in *LED-Based Photoacoustic Imaging*: Springer, 2020, pp. 133-158.
- [15] W. Fan, P. Moen, E. L. Kelly, L. B. Hammer, and L. F. J. J. o. v. b. Berkman, "Job strain, time strain, and well-being: A longitudinal, person-centered approach in two industries," vol. 110, pp. 102-116, 2019.
- [16] C. Champion, C. Kuziemy, E. Affleck, and G. G. J. I. J. o. I. M. Alvarez, "A systems approach for modeling health information complexity," vol. 49, pp. 343-354, 2019.
- [17] M. S. Ahmed, Y. T. AL-Tulaihi, and H. T. S. J. I. J. o. C. A. ALRikabi, "Bandwidth Analysis of a p- π -n Si Photodetector," vol. 975, p. 8887, 2016.
- [18] O. H. Yahya, H. Alrikabi, I. A. J. I. J. o. O. Aljazaery, and B. Engineering, "Reducing the Data Rate in Internet of Things Applications by Using Wireless Sensor Network," vol. 16, no. 03, pp. 107-116, 2020.
- [19] F. Wu, C. J. K. T. o. I. Liu, and I. Systems, "A Comprehensive and Practical Image Enhancement Method," vol. 13, no. 10, 2019.
- [20] L. Pan, M. Liu, and R. J. a. p. a. Hartley, "Single Image Optical Flow Estimation with an Event Camera," 2020.
- [21] I. A. J. J. o. U. o. B. Aljazaery, "Encryption of images and signals using wavelet transform and permutation algorithm," vol. 22, no. 9, pp. 2617-2634, 2014.
- [22] H. T. S. ALRikabi, A. H. M. Alaidi, F. T. J. J. o. A. R. i. D. Abed, and C. Systems, "Attendance System Design And Implementation Based On Radio Frequency Identification (RFID) And Arduino," vol. 10, no. 4, p. 6, 2018.
- [23] A. P. Chakkaravarthy, A. J. I. J. o. I. S. Chandrasekar, and Technology, "Anatomical region segmentation method from dermoscopic images of pigmented skin lesions," 2020.